

# Synthesis of Cr-Doped CaTiSiO<sub>5</sub> pigments by spray drying

T. Stoyanova Lyubenova<sup>1</sup>, F. Matteucci<sup>2</sup>, A.L. Costa<sup>2</sup>, M. Dondi<sup>2</sup>, M.Ocaña<sup>3</sup>, J. Carda<sup>1</sup>

<sup>1</sup>University Jaume I, Campus del Riu Sec, 12071 Castellon de la Plana, Spain

<sup>2</sup>Institute of Science and Technology for Ceramics, ISTECCNR, Faenza, Italy

<sup>3</sup>Institute of Materials Science (CSIC), Sevilla, Spain

---

**Abstract.** Cr-doped CaTiSiO<sub>5</sub> were synthesized by spray drying of an aqueous solution of precursor salts plus further calcining the resulting powders. The samples were prepared by conventional ceramic method as well for comparison study as ceramic pigments. The evolution of the present crystalline phases with applied thermal treatments has been studied by X-Ray Powder Diffraction (XRPD) and thermal analysis (DTA/TG). The powder morphology and particle size distribution were analyzed by scanning electron microscopy (SEM) and laser diffraction. The color efficiency of pigments was evaluated by colorimetric analysis (CIE Lab system). Results showed clearly efficiency of the spray dried procedure compared with the solid state reaction process. The produced powders consisted spherical particles with broad size distribution (<3µm), developing typical brown color. UV-VIS-NIR spectroscopy reveals the existence of Cr(III) as a majority phase occupies basically octahedral sites substituting Ti(IV), which must be responsible for the brown color of this pigment. Furthermore, Cr(IV) ions were found in octahedral coordination substituting Ti(IV) and small amount of tetravalent chromium substitutes for tetrahedral Si(IV).

**Keywords:** titanite, ceramic pigments, spray drying, color, crystallochemistry.

---

## 1. Introduction

Titanite (CaTiSiO<sub>5</sub>) is an orthosilicate accessory mineral in igneous and metamorphic rocks [1] and is topologically identical with well known Malayaite (CaSnSiO<sub>5</sub>)[2]. It has a good thermal stability and is recommended as excellent candidate for a host lattice of ceramic materials [3]. Since it is possible to incorporate a variety of elements into the crystal lattice [4], it has been used for immobilization of radioactive waste from nuclear power reactors [5], however as luminescent material [6].

Titanite structure is colorless, but become colored when the matrix is doped with transition metal cations, which act as chromophore agents as Cr(III). More in details, Cr -doped titanite possesses reddish brown shadows. Therefore, the local environment of the chromophore cation in the host matrix along with its oxidation state [7] and content [8] determine the optical properties of this pigment. However, the chromium is known as the most adaptable chromophore used in ceramic pigments due to its variety of oxidation states which produce various colors depending on the crystal field strength of a host matrix and synthesis procedure.

The transitional ion Cr(III) prefers octahedral environment than a tetrahedral one [9]. The titanite crystal structure consists of corner-sharing TiO<sub>6</sub> octahedra, connected via isolated SiO<sub>4</sub> tetrahedra to form TiOSiO<sub>4</sub> framework where the calcium ions are situated inside this network within very irregular heptacoordination, CaO<sub>7</sub> [10]. This six-fold coordination with

distorted symmetry caused by d-d transitions is desirable for red coloration. Ren and co-workers [9] established that in oxides as Malayaite ( $\text{CaSnSiO}_5$ ) chromium gives rise to pink, in Titanite ( $\text{CaTiSiO}_5$ ) develop brown shadows, maple in  $\text{TiO}_2$  and purple in  $\text{SnO}_2$ . The authors assumed that these colors are due to the Cr(III) and the Cr(IV) contain. Nevertheless, recently studies indicate that in malayaite structure the main phase is Cr(IV) responsible for the pink color of this pigments and the ion may reside in both octahedral and tetrahedral positions, while in Cr-doped  $\text{SnO}_2$  the essentially phase is Cr(III) developing violet shadows.[11]

Nowadays, many attempts have been carried on developing the most pure colors. The conventional synthesis of ceramic pigments is based on solid state reaction between oxide precursors and require higher firing temperatures with prolong retention times, addition of fluxing agents [12], who cause negative environmental effects [13], initial and fining grinding process [14]. Morphological characteristics and the final color of the pigments are not easy to produce due to existence of accessory phases [15]. Many authors have tried to develop pure and reproducible colors recurring to different synthesis methods, such as sol-gel [16-18], coprecipitation [19], combustion [20] and spray pyrolysis [21-23], hydrothermal [24]. However, due to the high cost of both raw materials and specific equipment necessary for the synthesis, no industrial application of these techniques has been developed up to now.

The aim of this work is to study the potential use of spray drying procedure as a non-convectonal method of synthesis for developing of Cr-doped titanite pigments, analyzing its thermal evolution, morphology, crystallochemistry and the optical properties.

## 2. Experimental Procedure

### 2.1. Powder preparation

Cr-doped titanite pigments were prepared by spray drying and traditional ceramic method (solid state reaction of oxides). The nominal compositions and the corresponding references of the samples prepared by both synthesis routs are detailed in Table 1.

### 2.2. Spray drying method.

The Cr-doped titanite samples were prepared by drying of liquid aerosols consisting of aqueous solution prepared by solubilizing of metal salts in the silica sol. The commercial silica sol Ludox PT-40 (Grace GMBH&Co.KG) was first purified in our laboratory by passing through a cation exchanging resin (Amberlite, Rohm and Haas) in order to remove the alkali-metal ion. The metal salts of  $\text{Ca}(\text{NO}_3)_2 \cdot 4\text{H}_2\text{O}$  (J.T Baker >99%) and  $\text{Cr}(\text{NO}_3)_3 \cdot 9\text{H}_2\text{O}$  (Aldrich, 99%), were added to the sol without previous dissolution. The titanium solution (0.32M) was firstly prepared by adding Titanium isopropoxide ( $\text{C}_{12}\text{H}_{28}\text{O}_4\text{Ti}$ , Aldrich, 97%) in a citric acid solution (2.5 mol/mol of titanium) in the presence of  $\text{H}_2\text{O}_2$  (2 mol/mol of Ti). The resulting red-brownish solution was then added to the precursor sol and the sol was basified at pH 6 with  $\text{NH}_4\text{OH}$ . This procedure was applied to avoid its decomposition in water. Simplified flow diagram of the described procedure is shown in the Fig.1

The precursor sols were spray-dried in a laboratory spray drier (Mod. SD-05, Lab-Plant Ltd.). The aerosol was generated by nebulization using air as a carrier gas with constant pressure. An inner jet nozzle was applied to introduce the starting solution into the expansion chamber, where the liquid droplets were dried into the chamber at  $220^\circ\text{C}$ . The resulting solid particles were collected in a glass bottle. The as-sprayed powders were

heated in an electric furnace at temperatures of 800°C, 1000°C, 1200°C with 4 hours of soaking time and heating rate of 200°C/hm in air.

### 2.3. Ceramic method.

The pigments were prepared using the traditional ceramic method with starting precursors as CaO (J.T Backer, 99%), SiO<sub>2</sub> (Strem Chemical 98%), TiO<sub>2</sub> (Strem Chemical, 98%) and Cr<sub>2</sub>O<sub>3</sub> (J.T Backer, 98%). For this, the stoichiometric amounts of the raw materials were mixed and homogenized with water by stirring. The powders were then dried (100±5°C) and further calcined for comparison study at 1200 with heating rate of 200°C/h and soaking time of 4h in air.

### 2.4. Characterization techniques

Differential thermal analysis (DTA) thermogravimetric (TGA) analysis were carried out in air using Mettler Toledo equipment, model TG/DTA 851e, along with the Mass spectra that was obtained simultaneously using Balzers Quadstartm 422. The thermogravimetric and differential curves were achieved in the range of 25°C-1500°C with a heating rate of 5° C min<sup>-1</sup>. The sample was heated in platinum crucible.

All the samples were characterized by X-ray diffraction (XRD) using Philips PW 1820/00 diffractometer at room temperature. The measurements were performed in the 15-90° 2θ range with Δ2θ step 0.02°, counting time per step 8s and the data were refined using the Rietveld method for the quantitative analysis (GSAS-EXPGUI) [25,26].

The morphology of the powders were examined by scanning electron microscopy (SEM, Cambridge StereoScan 360, Oxford ,UK). The samples were covered with a thin graphite layer by sputtering. The volumetric particle size distribution was obtained from laser diffraction measurement (Malvern MastersizeS).

UV-VIS-NIR spectroscopy (diffuse reflectance) of fired samples and their color coordinates were measured by Perkin Elmer Lambda 35 spectrophotometer in the 200-1400 nm range, step 0.1 nm, using BaSO<sub>4</sub> as a reference, D<sub>65</sub> as illuminant and 10° as observer. The colors were evaluated according to the Commission Internationale de l'Éclairage (CIE). The L\*a\*b\* parameters correspond: L\* is the color lightness (L\*= 0 for black, L\*=100 for white); a\* is red (+) and green (-) axis; b\* is the yellow (+) and blue (-) axis.

## 3. Results and Discussion

### 3.1. Structural characterization

The structural changes occur in the solids during their thermal treatment were studied by differential thermal and thermogravimetric analysis (Fig.2) coupled with simultaneously obtained mass spectra (Fig.3). The evolution of their phase composition was confirmed by X-ray diffraction technique. Both spray dried compositions presented almost identical behavior and as representative sample was taken SD1.

Thermogravimetric (TGA) and differential thermal analysis (DTA) obtain for the sample SD1 present series of endothermic and exothermic processes accompanied by total weight loss of 53,62%. The DTA curve show narrow endothermic peak at 61°C with weight loss of 18% in the range 25-150°C that could be attributed to the absorbed moisture during storage. The simultaneously scanned mass spectra shows ions with mass numbers M/e=17 and 18 corresponding to OH<sup>+</sup> and H<sub>2</sub>O<sup>+</sup> ions, which confirms the elimination of water. As well, in the DTA curve were noticed a broad endothermic peak at 511°C, which was related with weight lost of ~28% and mass numbers M/e=30 and 36. Therefore, the data were linked to NO<sup>+</sup> and NO<sub>2</sub><sup>+</sup> ions due to possible decomposition of nitrates. Further

mass lost of 2.3% were detected on the TGA curve in the interval 580-780°C. This effect could be associated with the titanite precursor decomposition, due to the combustion reaction of organic components. The mass spectra present ion currents with  $M/e=44$  attributed to  $\text{CO}_2^+$  and overlap with  $M/e=30$  and 46 that are matched the final step of nitrates decomposition.

At temperature above 800°C, no mass losses were detected on the TGA curve. An intense broad exothermic peak was observed in the DTA curve at 811°C and could be associated with the crystallization of more than one phase or transformation process. This theory was proofed by the X-ray diffraction (Fig.4), where at this temperature was observed the crystallization of two phases: titanite  $\text{CaTiSiO}_5$  ~79% wt (ICSD N°50280) and perovskite  $\text{CaTiO}_3$  ~21 % wt (ICSD N°97828). A further increasing of the firing temperature up to 1000°C raised the amount of titanite to 89% wt, but still presented the perovskite crystalline phase. The present of the two phases was confirmed by the double hill peak at 1081°C. The perovskite phase is thermodynamically unstable at high temperatures and probably its decomposition provokes titanite crystal growth. Finally, at 1200°C titanite reaches 98% wt as a mayor crystalline phase.

Parallel X-ray diffraction result was obtained for the sample SD2 calcined at the same temperatures (Figure 5). In this pattern elevated crystallinity and bigger amount of perovskite reflection was observed at  $2\theta\sim 33.5$ . In order to obtain completely pure crystalline phase the spray dried samples were calcined at 1300°C, but were melted.

On the other hand, the thermal evolutions of the samples, prepared by the traditional ceramic method and calcined at 1200°C demonstrated variety of crystal phases (Fig.6). Only one quantitative refinement was made for the sample C1 as well, because of the high number of crystalline phases. The representative sample contain the following weight amounts: 33% of  $\text{CaTiSiO}_5$ , 45% of perovskite  $\text{CaTiO}_3$ , 10% of  $\text{SiO}_2$  as quartz (ICSD N°9276) and 12% of cristobalite (ICSD N°47220).

In order to study the influence of the chromium amount the diffraction results of the titanite doped with 2wt. % and 5wt.% of chromium were compared. The results (Fig.7) showed a displacement of the diffraction peaks up to the major angles  $2\theta$  in all the samples. This phenomenon is usually associated with reducing of the unit cell parameters according to the replacement of an ion by a smaller one. However, the interpretation is more complicated since chromium is found in different positions and oxidation states according to UV-VIS-NIR results.

Baring in mind the ionic radius data proposed by Shannon [27] two assuming are possible: a) tetrahedral  $\text{Cr}^{4+}$ (0.55Å) to be incorporated instead of  $\text{Ti}^{4+}$ (0.745Å) in octahedral positions and b) octahedral  $\text{Cr}^{4+}$ (0.69Å) to substitute  $\text{Ti}^{4+}$ (0.745Å) sites. Both assume can be solutions for the observed diffraction displacement. In addition, it is possible  $\text{Cr(III)}$  to replace  $\text{Ti(IV)}$  in octahedral position by an oxygen vacancy mechanism [in private communication M.Dondi] This assumes is a further problem and can not be resolved by the experimental data that was carried out in the present study.

In conclusion, the advantages provided by spray drying road in order to obtain better titanite formation are obvious. The technological benefits are decreasing the firing temperature, increasing the homogeneity of the powders as well as size and particle distribution control, which was already demonstrated [28, 29].

### 3.2. Microstructural characterization.

The microstructure of the as-prepared spray drying sample SD1 (chosen as a representative) is shown in Fig8 (a). It is observed spherical hollow particles with diameters ranging from 0.5 to 5  $\mu\text{m}$  and broad size distribution. However, the calcined at 1200°C pigments (Fig 8b) were not significantly altered. Besides can be observed

irrelevant coagulation process, which is probably due to higher initial droplet concentration. Moreover the particle dimensions are below than 10 $\mu\text{m}$  which is sufficiently small for their direct application in the ceramic glazes. It can be pointed out in the representative case of the sample C1 that consist very sintering agglomerates with irregularly shaped and huge dimensions. The aggregates exhibit a broader size distribution due to the higher solids contents of the feeding material (Fig.8c)

The volumetric curve of the both samples is shown in the Fig 8d. As it is illustrated the mean particle size of spray dried pigment was much smaller than ceramic one. It possesses two maxima centers at 0.3 $\mu\text{m}$  and 3 $\mu\text{m}$ . Besides, the sample prepared by ceramic rout possess strongly displaced second maxima center at 30 $\mu\text{m}$ .

In order to study the chromophore surrounding all synthesized sample were analyzed by UV-VIS-NIR. The corresponding absorption spectra are shown in Fig 9.

In general, the spectra present similar features and can be explain by the ligand field theory [30]. According to this theory, the chromopher Cr(III) ion in an octahedral environment predict existence of three absorption bands. The energy of the first two electronic transitions,  ${}^4A_2 \rightarrow {}^4T_2$  and  ${}^4A_2 \rightarrow {}^4T_1$  (F), correspond to the visible part of the electromagnetic spectrum. In this region appear absorption band at 480 nm (in SD1 spectra), at 380 nm (in SD2) and at 409 nm (in C2). These bands can be attributed to the second allowed Cr(III) transition  ${}^4A_2 \rightarrow {}^4T_1$  (F). Similar band are observed in the garnet [31] and cassiterite structures [9, 22]. The third spin allowed transition  ${}^4A_2 \rightarrow {}^4T_1$  (P) appears in the ultraviolet region and even does not affect the color is presented in our spectra by 236 nm and 290 nm. It is also detected another band at 760nm which is stronger in the ceramic samples. This band can not be related with the first electronic spin allowed transition  ${}^4A_2 \rightarrow {}^4T_2$ , which appears around 600nm. In fact, the titanite structure is a host oxide with distorted octahedral symmetry, thus can origin spin-forbidden transitions between the excited state  ${}^2E$  and the fundamental state  ${}^2A_2$ , called R lines. These lines appear approximately at 690 nm and have already discussed by authors [7, 32]. It is necessary to indicate that the intensity of the absorption peaks increases with the chromium concentration.

In the optical absorption of SD2 sample exists a broad band at 511nm which is mainly attributed to Cr (IV) cation in distorted octahedral coordination that correspond to the spin allowed transition  ${}^3T_1 \rightarrow {}^3T_2$  [33]. This broadening seems to be caused by the overlapping of Cr(III) and Cr(IV) spectra that have been discussed [9]. As well, a strong band at 1150nm in the near-IR part of the spectrum was observed which was previously found in the malayaite structure [11]. This band can be associated with the  ${}^3A_2 \rightarrow {}^3T_1$  electric dipole allowed transitions of Cr (IV) in tetrahedral coordination.

As a conclusion, the chromium chromopher in the Cr-doped titanite structure is presented by two main oxidation states. The major part is presented from Cr(III) who occupy octahedral Ti(IV) sites. Although, part of the total chromium content may be substituted of Cr(IV) in tetrahedral Si(IV) position and very small amount in the SD2 sample occupy octahedral Ti(IV) positions.

Therefore, the brown color that develops in the samples can be due to the combination of Cr(III) and Cr(IV) oxidation states presented in the Cr-doped titanite pigments.

### 3.3. Color coordinates

The color parameters CIE  $L^*a^*b^*$  [34] of all the samples at different calcinations temperature are shown in Table 3. It is emphasis to the evolution of the representative spray drying sample SD1. It can be seen, that the as- prepared sample is almost colorless (negative  $a^*$ , high  $b^*$  and very high luminosity corresponding to the  $L^*$  value). The match shade is yellow. Among further calcination at 800 $^\circ\text{C}$  the pigment presents already light

brown shadow, which increases its intensity with rising of the calcining temperature. These changes involved the appearing of a light brown color, which progressively turned to darker brown on a further heating up to 1200°C. It should be noted that with a certain increase of the chromium content (as in SD2) it was not detected expected increasing of the coordinate  $a^*$ . The same evolution is distinguished in their ceramic equivalents. The luminosity  $L^*$  present almost irrelevantly changes, keeping average values at high temperatures. The most intensive brown shade possesses the sample SD1 doped with 2 wt% of chromium.

#### 4. Conclusion

The spray drying method proved to be suitable to get almost pure titanite with improved characteristics for applications as ceramic pigment, with respect to the conventional ceramic process. The developed powders are more reactive, leading to a purer pigment at lower firing temperature. Its small grain size and regular particle distribution avoids any final milling and mineralizer additives. All Cr-doped titanite pigments develop brown shades due to the combination of Cr(III) and Cr(IV) oxidation states. The most intensive brown shade possesses the sample SD1 doped with 2 wt% of chromium. The spray drying technique is also feasible due to its simplicity and current use in the ceramic tile industries.

#### Acknowledgements

The author (T.S.L.) would like to acknowledge the financial support provided by the Spanish Ministry of Science and Education under the project of (FPU) for the realization of PhD research at the University JAUME I of Castellón (Spain) and a temporary stay at the Institute of Science and Technology for Ceramics (Faenza, Italy).

#### References

- [1] Frost BR, Chamberlain KR, Schumacher JC "Sphene (titanite): phase relations and role as a geochronometer", *CHEMICAL GEOLOGY* 172 (1-2): 131-148 Sp. Iss. SI, FEB 1 2001
- [2] JOHN B. HIGGINS AND PAUL H. RIBBE, "The structure of malayaite,  $\text{CaSnOSiO}_4$ , a tin analog of titanite", *American Mineralogist*, Volume 62, pages 801-806, 1977
- [3] Malcherek T, Domeneghetti CM, Tazzoli V, Salje EKH, Bismayer U, "A high temperature diffraction study of synthetic titanite  $\text{CaTiOSiO}_4$ " *PHASE TRANSITIONS* 69 (1): 119-131 Part B, 1999
- [4] Dondi M, Matteucci F, Cruciani G Zirconium titanate ceramic pigments: Crystal structure, optical spectroscopy and technological properties, *JOURNAL OF SOLID STATE CHEMISTRY* 179 (1): 233-246 JAN 2006
- [5] P.J Hayward, W. Lutze, R.C Swing, *Radioactive Forms for the Future*, p.427, Elsevier, Amsterdam (1988)
- [6] Laser-induced time-resolved luminescence of natural titanite  $\text{CaTiOSiO}_4$ , M. Gaft a\*, L. Nagli b, R. Reifeld c, G. Panczer d, *Optical Materials* 24 (2003) 231-241
- [7] R.S. Pavlov, V.B. Marzá, J.B. Carda, Electronic absorption spectroscopy and color of chromium-doped solids, *J. Mater. Chem.* Vol.12 (2002) p.2825.
- [8] E. López-Navarrete, M.Ocaña, "A simple procedure for the preparation of Cr-doped tin sphene pigments in the absence of fluxes", *J. Eur. Ceram. Soc.*, Vol. 22 (2002) p.353-359.
- [9] Ren Feng, Ishida Shingo, Takeuchi Nobuyuki, Fujiyoshi Kaichi, Chromium- Based Ceramic Colors, *Ceram Bull.*, n.5, vol.71, 1992
- [10] J. Alexander Speer, G.V Gibbs, "The crystal structure of synthetic titanite,  $\text{CaTiOSiO}_4$ , and the domain textures of natural titanites", *American Mineralogist*, Volume 61, pages 238-247, 1976
- [11] E.Lopez Navarrete, A.Cballero, V. M Orera, F.J Lázaro, M.Ocaña, Oxidation State and localization of chromium ion in Cr-doped cassiterite and Cr-doped Malayaite, *Acta Materialia*, 51, 2003, 2371-2381
- [12] E.Cordoncillo, F.del Rio, J.Cardá, M.Llusar, P.Escribano, "Influence of some mineralizers in the synthesis of sphene-pink pigments", *J.Eur.Cer.Soc.*, 1998, 18, 1115-1120

- [13] Llusar, M. & Badenes, J.A. & Calbo, J. & Tena M.A. & Monrós, G., Environmental optimization of flux additions. *Am.Cer. Soc.Bull.*, 1999, 78(7), pp. 63-8
- [14] Decker, C.T., Effects of grinding on pigment strength in ceramic glazes. *Ceram.Eng.Sci.Proc.*, 1992, 13(1-2), pp. 100-8
- [15] Cordoncillo, E.& del Rio, F. & Carda, J.B. & Llusar, M. & Escribano, P., Influence of some mineralizers in the synthesis of sphene-pink pigments. *J. Eur. Ceram. Soc.*, 1998,18 (8), pp. 1115-20
- [16] Ou-benmou, I.& Ahamdane, H. & El idrissi Raghni, M.A & Bensamka, F.& Mosset, A., El idrissi Moubtasim, M.L.& Jumas, J.C., Tin sphene-sized powders. *J. Eur. Ceram. Soc.*, 2000, 20, pp. 2159-63
- [17] Monros, G. & Carda, J. & Tena, M.A. & Escribano, P. & Sales, M. & Alarcon, J., Synthesis and characterization of  $V_2O_5$ - $SiO_2$ - $ZrO_2$  pigments by sol-gel method. *J. Non-Cryst.Solids*, 1992, 147, pp.588-93
- [18] Carda, J. & Monros, G. & Escribano, P. & Alarcon, J., Synthesis of uvarovite garnet. *J. Am. Ceram. Soc.*, 1989, 72 (1), pp.160-62
- [19] Stefani, R.& Longo, E.& Escribano, P.& Cordoncillo, E.&Carda, J., Developing a Pink Pigment for Glazes. *Am. Ceram. Soc. Bull.*, 1997, 176 (9), pp.61-64
- [20] Muthuraman, M. & Patil, K.C., Synthesis, properties, sintering and microstructure of sphene,  $CaTiSiO_5$ : A comparative study of coprecipitation, Sol-gel and combustion process. *Mat.Res.Bull.*, 1998, 33 (4), pp. 655-61
- [21] E. López-Navarrete, V. Orera, F.J.Lázaro,J.B.Cardá, M.Ocaña "Preparation through aerosols of Cr-doped  $Y_2Sn_2O_7$  (Pyrochlore) Red shade pigments and determination of the Cr oxidation State",*J.Am.Cer.oc*, 87[11]2108-2113(2004)
- [22] E. López-Navarrete, A.R. González-Elipe, M. Ocaña, "Non-conventional synthesis of Cr-doped  $SnO_2$  pigments",*Ceramics International* 29 (2003) 385–392
- [23]L. G. Messing,, Zhang Shi-Chang, V. Gopal Jayanthi: Ceramic Powder Synthesis by Spray Pyrolysis., *J. Am. Ceram. Soc.*, **76** (11), (1993), 2707-26
- [24] Bondioli, F. & Leonelli, C. & Manfredini, T., Microwave-hydrothermal synthesis and hyperfine characterization of oraseodymium-doped nanometric zirconia powders. *J. Am. Ceram. Soc.*, 2005, 88 (3), pp. 633–38
- [25] Larson, A.C. & Von Dreele, R.B., GSAS: General Structure. Analysis System. Los Alamos Nat. Lab. Report LAUR, 1994, pp. 86-748
- [26] Toby, B.H., EXPGUI, a graphical user interface for GSAS. *J. Appl. Cryst.*, 2001, 34, pp. 210-13
- [27] Shannon R D,*Acta Crstallogr*, 1976,A32,751-767
- [28] Costa, A. & Galassi, C. & Roncari, E., Direct synthesis of PMN samples by spray drying, *J. Eur. Ceram. Soc.* 2002, 22, pp. 2093-100
- [29] Costa, A. & Galassi, C& Roncari, E., Spray-drying derived lead magnesium niobate perovskite ceramics. *Euro ceramics VII*, *Key Eng.Mat.*, 2002, 206 (2), pp. 171-74
- [30] Marfunin A.S., *Physicsof Minerals and Inorganic Materilas*, Springer-Verlag, Berlin Heidelberg New York, 1979
- [31] New pink ceramic pigment basaed on chromium (IV)-doped lutetium gallium garnet, R.Galindo, M.Llusar, M.A Tena, G.Monrrós, J.A Badenes, *Journal of Eurpean Ceram Soc*, 27 (2007), 199-205
- [32] Y.Marinova, J.M Hohemberger, E. Cordoncillo, P.Escribano, J.B Carda, Study of solid solutions, with perovskite structure, for application in the field of the ceramic pigments, *Jour.Europ.Cer. Soc*, 23 (2003), 213-220
- [33] Tanabe Y., Sugano S., On the absorption spectra of complex ions II, *Journal of the Physical Society of Japan*, vol.9,n.5,sept-oct,1954
- [34] Commission Internationale del'Eclairage, " Recommendations and Uniform Color Spaces, Color Difference Equations, Phychomet rics Color Terms", Supplement n.2 of CIE Publication No. 15(E1-1.31);1971 (Bureau Central de la CIE, Paris,1978)

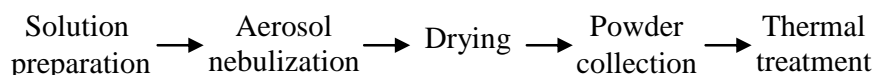


Fig 1. Flow diagram of the spray drying procedure

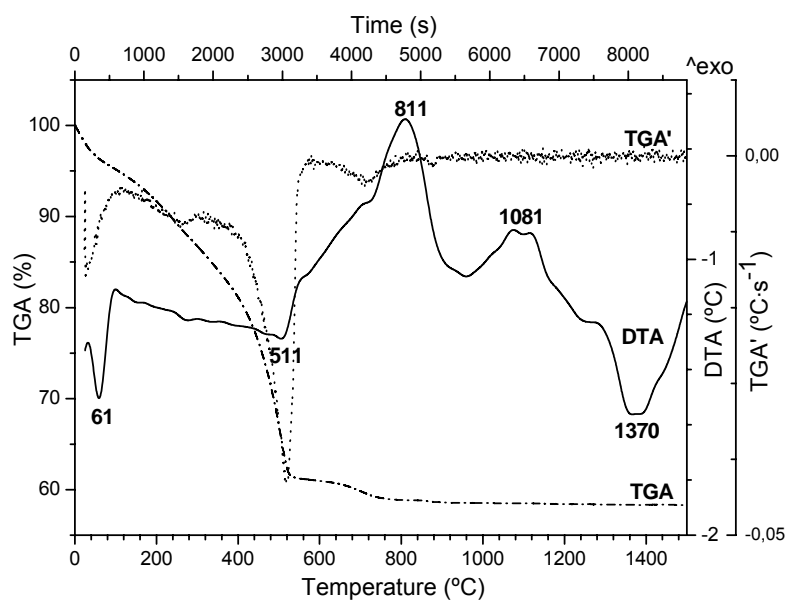


Fig 2. Differential thermal (DTA) and thermogravimetric (TGA) analysis curves obtained for sample SD1

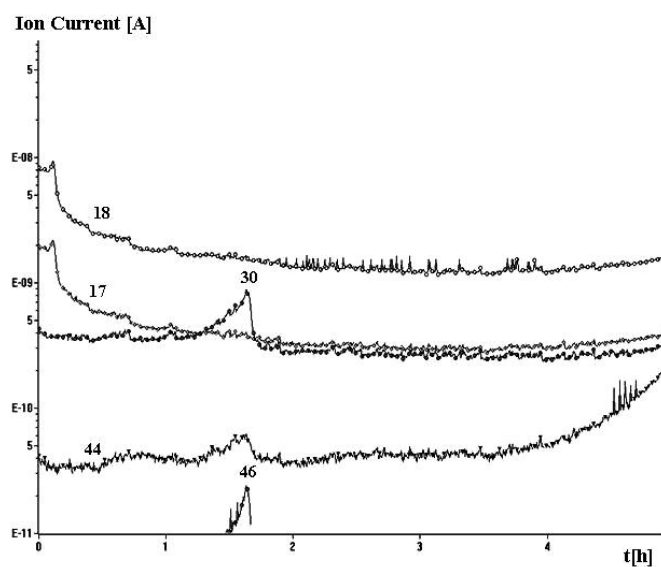


Fig 3. Mass spectra of the ions with  $M/e=17, 18, 30, 44,$  and  $46$  scanned simultaneously with the TGA/DTA of the sample SD1



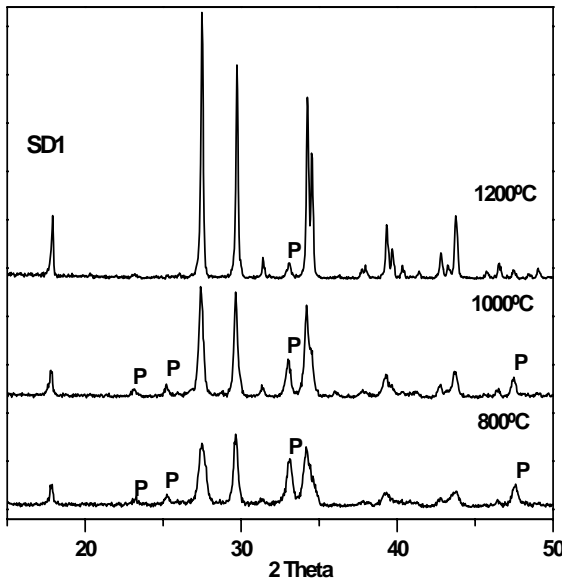


Figure 4 . X-ray diffraction patterns obtained for sample SD1 after heating for 4h at different temperatures. Symbols: (P-CaTiO<sub>3</sub>; The titanite peaks have not been labeled.

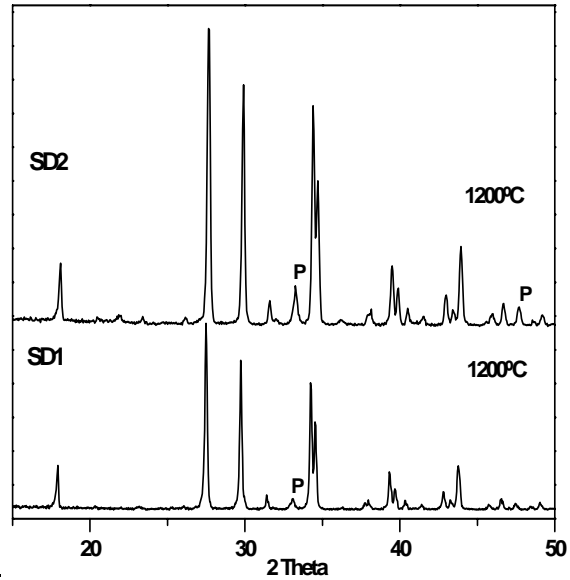


Figure 5 . X-ray diffraction patterns obtained for sample SD1 and SD2 after thermal treatment at 1200°C with retention of 4h. (P-CaTiO<sub>3</sub>). Titanite peaks have not been labeled.

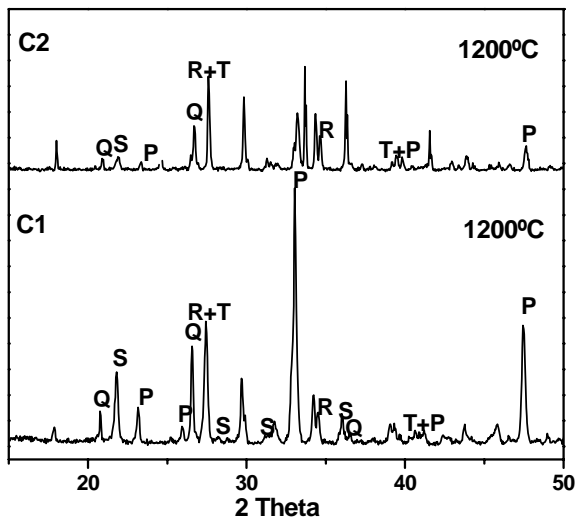


Fig. 6 X-ray diffraction patterns obtained for sample C1 after thermal treatment at different temperatures with retention of 4h. (P-CaTiO<sub>3</sub>, Q-SiO<sub>2</sub>(quartz); S- SiO<sub>2</sub>(cristobalite), R-TiO<sub>2</sub>. The pure Titanite CaTiSiO<sub>5</sub> peaks have not been labeled

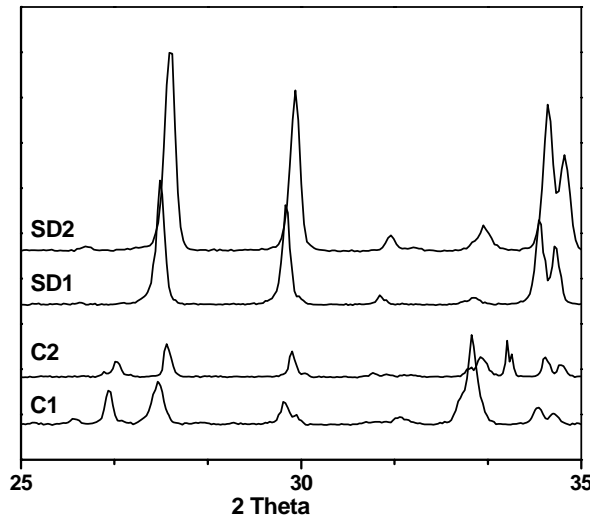


Fig.7 X-ray Diffraction peaks, displaced by the incorporation of chromium.

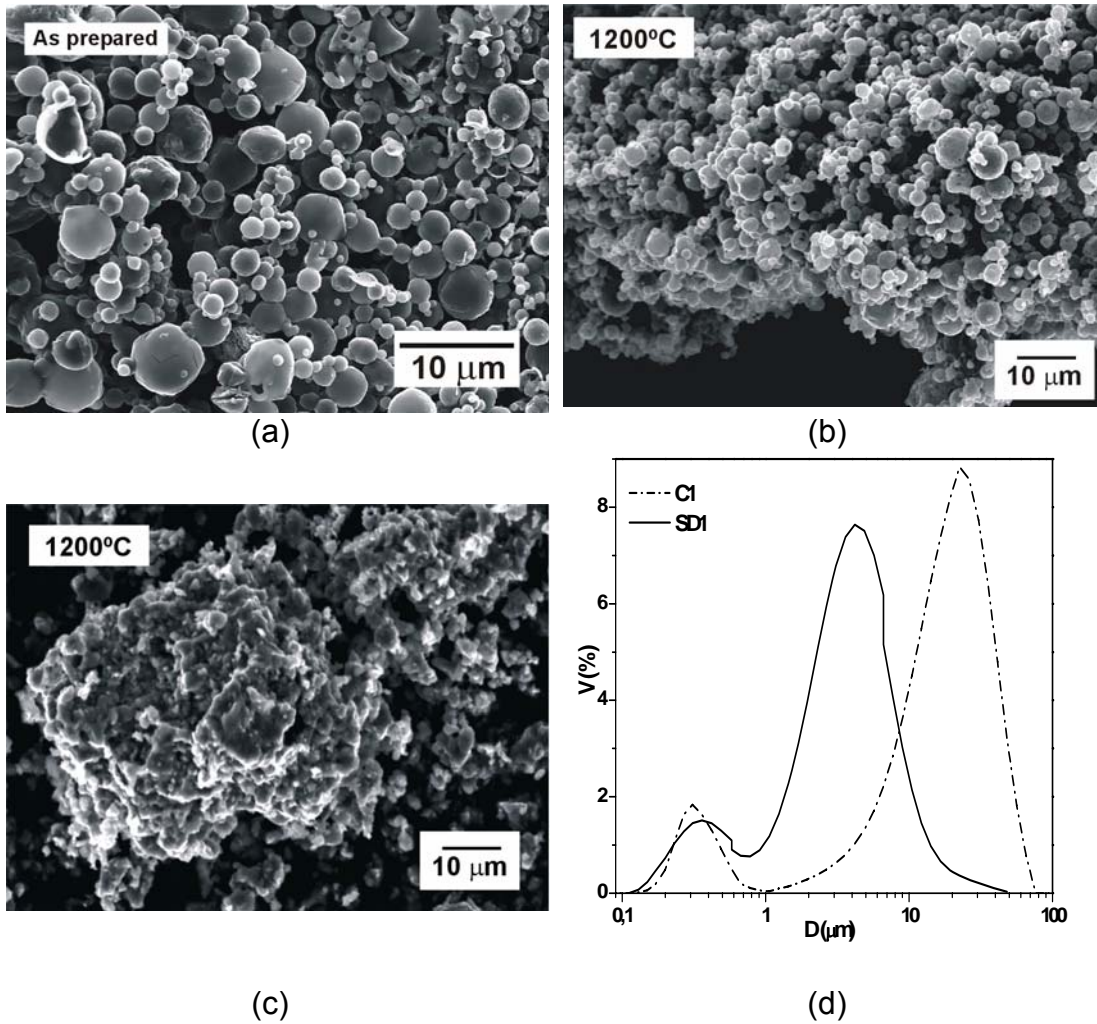


Fig.8. Scanning electron micrographs: (a) as prepared SD1; (b) SD1-after heating at 1200°C, (c) C1-after heating at 1200°C and (d) is volumetric particle size distribution

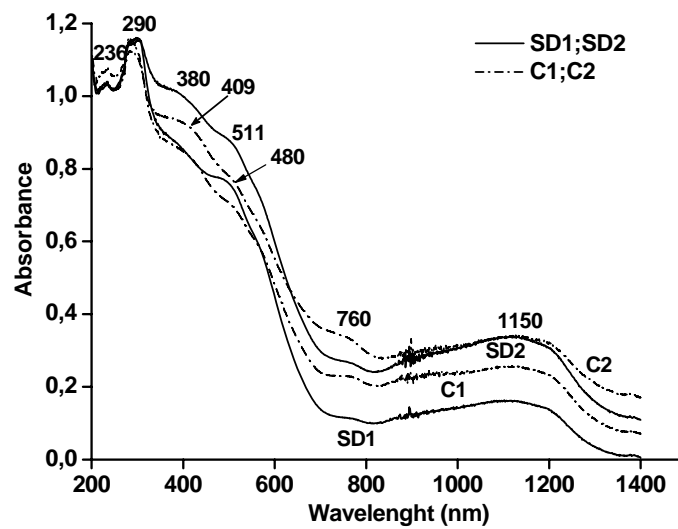


Fig 9. Optical absorption spectra obtained for Cr-doped titanite heated at 1200°C for 4h: 1-SD1; 2-C1; 3-C2; 4-SD2

Table1. References and studied samples

Composition	Synthesis method and sample references	
	Ceramic	Spray drying
<b>CaTi<sub>0.98</sub>Cr</b>	C1	SD1
<b>0.02SiO<sub>5</sub></b>	C2	SD2
<b>CaTi<sub>0.95</sub>Cr</b>		
<b>0.05SiO<sub>5</sub></b>		

Table 2.  $L^*a^*b^*$  parameters measured for the as prepared spray dried sample and after thermal treatment at different temperatures.

Sample	Temperature (°C)	$L^*$	$a^*$	$b^*$	Color
As-prepared SD1	220	93.5	-6.3	16.7	yellow
SD1	800	82.7	3.4	7.9	Light burlywood
SD1	1000	74.1	10.9	15.5	Light brown
<b>SD1</b>	<b>1200</b>	<b>64.4</b>	<b>20.7</b>	<b>21.5</b>	<b>Brown</b>
SD2	1000	66.4	12.9	12.1	Burlywood
SD2	1200	65.7	16.9	20.7	Brown
C1	1200	68.7	14.4	19.2	Brown
C2	1200	71.3	12.7	31.3	Brown